Title: *Impairments of* saccadic and reaching *adaptation in Essential Tremor are linked to movement execution*

Abbreviated title: *Motor adaptation impairments in Essential Tremor*

Florence Blondiaux – 1 & 2

Louisien Lebrun – 2 & 3

Bernard J. Hanseeuw – 2, 3, 4 & 5

Frédéric Crevecoeur – 1 & 2

Institute for Information and Communication Technologies, Electronics and Applied Mathematics, UCLouvain, Avenue Georges Lemaitre 4-6, 1348 Louvain-la-Neuve, Belgium

1- Institute of Neuroscience, UCLouvain, Avenue E. Mounier 53, 1200 Brussels, Belgium
2- Neurology Department, Saint-Luc University Hospital, Avenue Hippocrate 10, 1200 Brussels, Belgium
3- Gordon Center for Medical Imaging, Radiology Department, Massachusetts General Hospital, Harvard Medical School, MA 02114-1107, Boston, USA
4- Louvain Aging Brain Lab, Walloon Excellence in Life Sciences and Biotechnology (WELBIO), UCLouvain, Avenue E. Mounier 53, 1200 Brussels, Belgium.

Corresponding author: Frédéric Crevecoeur – frederic.crevecoeur@uclouvain.be

Conflict of interest statement: The authors declare no competing financial interests.

Acknowledgments: Florence Blondiaux is a FRIA grantee of the Fonds de la Recherche Scientifique – FNRS (Be). The FNRS provided salary and research support for Bernard Hanseeuw under grants n° CCL40010417 and n° FRFS-WELBIO40010035. Frédéric Crevecoeur is supported by a grant from the FNRS under grant number 1.C.033.18.

0. Abstract

Essential tremor (ET) is a neurological disorder characterized by involuntary oscillations of the limbs. Previous studies have hypothesized that ET was a cerebellar disorder and reported impairments in motor adaptation. However, recent advances have highlighted that motor adaptation involved several components linked to anticipation and control, all dependent on cerebellum. We studied the contribution of both components in adaptation to better understand the adaptation impairments observed in ET from a behavioural perspective. To address this question, we investigated behavioural markers of adaptation in ET patients (n=20) and age-matched neurologically intact volunteers (n=20) in saccadic and upper limb adaptation tasks, probing compensation for target jumps and for velocity-dependent force fields, respectively. We found that both groups adapted their movements to the novel contexts, however, ET patients adapted to a lesser extent compared to neurologically intact volunteers. Importantly, components of the movement linked to anticipation were preserved in the ET group, whereas components linked to movement execution appeared responsible for the adaptation deficit in this group. Altogether, our results suggest that execution deficits may be a specific functional consequence of the alteration of neural pathways associated with ET.

New & Noteworthy: We tested Essential Tremor patients' adaptation abilities in classical tasks including saccadic adaptation to target jumps and reaching adaptation to force field disturbances. Patients' adaptation was present but impaired in both tasks. Interestingly, the deficits were mainly present during movement execution, while the anticipatory components of movements were similar to neurologically intact volunteers. These findings reinforce the hypothesis of a cerebellar origin for essential tremor and detail the motor adaptation impairments previously found in this disorder.

1. Introduction

Essential tremor (ET) is one of the most common movement disorders provoking involuntary oscillations of patients' limbs (1). Typical clinical features of ET are kinetic and intention tremors of limbs, particularly upper limbs and, to a lesser extent, head and trunk (2–4). To date, the pathophysiology of this neurological disorder is not fully understood, but some previous works have suggested a cerebellar origin (5). Neuroimaging studies reported abnormalities in the structure and connectivity of cerebellum as well as differences in the cerebello-thalamo-cortical loop (6–9). Postmortem studies also pointed towards alterations of cerebellar cells (10). Characterizing whether specific cerebellar functions are preserved or impaired in this condition is therefore important to better understand this disorder.

Crucial functions of cerebellum include movement control, state-estimation, and adaptation (11–13). The central nervous system cannot exactly access the state of the limbs (position, speed, etc.) due to the intrinsic delays in sensory feedback and to sensorimotor noise. As a result of this uncertainty, the brain must predict the next state that will be used to plan and control fast and accurate movements. The prediction is computed based on the delayed sensory feedback and an efferent copy of the motor command used in conjunction with prior knowledge of body and environmental dynamics. This operation of state estimation, which makes use of internal models, has been associated with cerebellum (14–17).

The ability to adapt motor patterns to novel environments rests on our ability to update the internal models used for estimation and control, thereby allowing for predictive compensation for sustained disturbance. It has been reported that adaptation depends on the integrity of cerebellum. The involvement of cerebellum in motor adaptation has been studied with a variety of movements, with non-human species (18, 19), as well as with cerebellar patients (20–22), who have shown deficits of adaptation in response to repeated perturbations. These results possibly reflect inaccurate internal models and a relative inability to update them in a way that counters the disturbance induced by the novel environment (11, 13).

Given the involvement of cerebellum in sensorimotor adaptation and its putative link with tremor, we set out to describe motor adaptation impairments in ET across two different tasks. Previous works reported that these patients were able to adapt to perturbations, but to a lesser extent than neurologically intact volunteers in force-field, visuomotor and prism adaptation tasks, as well as eyeblink conditioning (23–26). Considering that sensorimotor adaptation may involve multiple components (27), we aimed to expound this adaptation deficit using two tasks probing

visual and upper limb motor systems. In particular, we focused on the contributions of anticipation and movement execution on motor adaptation deficits. To do so, we studied adaptation in saccadic eye movements evoked by peri-saccadic target jumps, and upper limb reaching adaptation to velocity-dependent force fields as well as the correlation of adaptation performances in both tasks. We found that motor adaptation deficits observed in both tasks were due to the time course of movement execution while anticipatory compensation for the perturbation was comparable to the control group.

Our results support the hypothesis of a cerebellar origin for essential tremor but suggest a specific alteration of the pathways linked to the real-time motor execution across both visual and upper limb motor systems.

2. Methods

Participants

A total of 22 Essential Tremor (ET) patients and 20 neurologically intact (NI) volunteers participated in this study. All participants provided written informed consent following procedures approved by the Ethics Committee at the host institution (*Comité d'Éthique Hospitalo Facultaire*, UCLouvain, Belgium). A neurologist performed a clinical evaluation with the Fahn-Tolosa-Marin Tremor Rating Scale (FTM-TRS) (28) on all participants to evaluate the severity of the tremor. ET patients did not interrupt their medication before the assessment. We kept track of current medications and dosages (Supplementary Table 1). All but four ET participants took part in the two experiments. For the reaching experiment, one participant could not perform the task due to the amplitude of their hand tremor, another participant did not complete the task due to pre-existing shoulder condition. For the saccadic adaptation experiment, two other participants were excluded following technical limitations impeding calibration of the eye-tracking system. As a result, each population of ET patients was composed of 20 volunteers. Force sensors were defective for one ET participant, and another ET participant decided to stop the experiment a block earlier. We kept the data for the analyses and took into account the missing trials and the absence of force recordings. All NI volunteers participated in the two tasks, resulting in a group of 20 NI volunteers.

The FTM tremor rating scale was divided into three sections. Part A quantified the tremor amplitude of the limbs at rest, with posture holding, and during action. Part B quantified the action tremor of the upper limbs, particularly writing, drawing, and pouring liquids. Part C quantified the functional disability, evaluating patients' impairments in daily life activities (eating, drinking, working, etc.). We ignored this part filled by the participant due to the higher subjectivity of some

criteria and because our experiments assessed different tasks. Maximum scores for each section were respectively, 80, 32, and 28. Since this scale is not specific to ET evaluation, a low score in some items is expected like rest tremor, uncommon in ET.

Tasks

The study was composed of two experiments: a saccadic adaptation task (Figure 1&2) and a reaching adaptation task to a force field (Figure 3&4). During the saccadic adaptation task inspired from Xu-Wilson et al. (22), participants sat in a dark room on a height-adjustable chair in front of a screen. Head movements were restricted using a chin rest bar and forehead support. Eye movements were recorded using an Eyelink 1000 Tower-mounted eye tracker (SR Research, Ottawa, Canada) at a sampling rate of 1kHz, and stored for offline analyses. Participants gazed at the green targets (0.8 visual degrees wide) displayed on the screen. After a series of baseline trials containing a fixation target and a goal target, a jump of the goal target was introduced as a perturbation for the adaptation trials (Figure 1a&b). We divided the experiment into 7 blocks: oblique (30 trials), horizontal (30 trials), and five adaptation blocks (60 trials each). Coordinates are expressed in degrees of visual angle both for the horizontal and vertical component, with the center (0°,0°) being straight ahead of the participants.

During the oblique trials, a fixation target (F: (-10°,0°)) was projected on the left side of the screen. After a random wait time between 2 sec and 3 sec distributed uniformly, a new target was projected 20° away from the fixation target in the horizontal direction and 5° above the meridian vertically (T1: (10°,5°)). For the horizontal trials, the same fixation target (F) was used, and the final target was 20° away in the horizontal direction but aligned vertically (T1: (10°,0°)). We refer to the initial measurements of oblique and horizontal trials as *baseline* trials. The adaptation trials started with the same initial fixation target (F). A second target displayed 20° to the right appeared (T1: (10°,0°)), and participants were instructed to direct their gaze to the new target. As soon as the saccade was detected, the target jumped 5° away in the vertical direction (T2: (10°,5°)). The target T2 served as a fixation target for the next trial, the jump continued to be counterclockwise (F = (10°,5°); T1: (-10,5°); T2: (-10,0°)). See Figure 1a&b for a sketch of the different targets coordinates. The saccades were detected based on a horizontal velocity threshold of 150°/s computed online using backward 2nd order finite differences. Because of the perturbation, the saccade towards T1 was followed by a corrective saccade towards T2. An inter trial time of 2.3sec was used in all cases. Participants took a short break between each block (15sec to 1min).

For the reaching adaptation task, participants sat on a height-adjustable chair in front of an End Point KINARM device (KINARM, Kingston, Ontario). They grabbed the handle of the robotic arm and performed reaching movements toward the target projected on the screen (Figure 3a). All participants performed the experiment with their right arm, independently of their laterality based on recent observation that adaptation on each side for the same task is very similar (29). The device recorded the participants' hand cursor position and forces applied to the handle. An occluder blocked the direct vision of the hand, but a hand-aligned cursor was always represented (white dot, radius 0.6 cm). The radius of the targets was 1.2 cm. A criterion on movement time was applied to encourage consistent velocities, but all movements crossing the target at least once and finishing within less than 3 cm from its center were kept for analyses. Good movement time ([600 ms – 1500 ms]) was indicated by a green target at the end of the trial. If the participant was too slow, the target remained red and full. For movements too quick, the target switched to red and hollow. The experiment was composed of two trial types: null-field trials, and force field trials. During the null-field block (40 trials), participants were instructed to reach and stop at the displayed target. Two goal targets were used to avoid potential bias liked to the repetition of one target and to make the task less repetitive. The two goal targets and the start target formed an equilateral triangle. Targets centers were 10 cm apart. The start target, closest to the participant, was aligned with their elbow. For each trial, one of the two possible goal target was randomly selected and displayed on the screen. Each set was composed of the same number of trials towards each target. The adaptation blocks (4 blocks) featured trials with similar instructions but performed in the presence of a clockwise velocity-dependent curl field applied throughout the whole movement. The force field was defied as followed: $f_x = 15\,\dot{y}$ and $f_y = -15\,\dot{x}$ (N). Each block was composed of 66 trials: 30 trials towards each target with the force field, and 3 catch trials per target during which the force field was unpredictably turned off. The trials were presented in random order. The inter-trial time was 1sec. Participants were encouraged to take short breaks between the blocks to reduce fatigue (15 sec to 1 min).

Data Analysis

Raw measurements of eye position were filtered with a dual-pass 4th order low pass Butterworth filter with a cut-off frequency of 50 Hz. Eye velocity was computed based on position signals using 4th order finite differences. The beginning and end of each saccade were defined using a threshold on the horizontal eye velocity of 16°/s for at least 10 ms. Additional criteria for saccade inclusion were: (1) its duration, within 50 to 200 ms, (2) its peak velocity, above 100°/s, and (3) a

minimum amplitude of 10°, corresponding to one-half of the instructed horizontal displacement. These inclusion/exclusion criterions were adapted from (22). On average, NI volunteers had 11.7% of their trials excluded (min: 3.9%, max: 38.9%), ET patients 14.7% excluded (min: 3.9%, max: 31.4%). Non-detected saccades were mainly due to blinks and fatigue leading to poor detection of the pupil by the eye-tracking system. The mean velocity was computed on a 40ms window, centered around the trial's peak velocity. The curvature of saccades was approximated using the same method as Chen-Harris and colleagues (30). Each saccade was divided into 4 equal segments along the horizontal direction, the slope of the line extending the end of each segment was computed and was referred to as S1-S4 (see Figure 2c-g). The timing of each segment was in average 21.7ms, 11.8ms, 13.2ms and 28.5ms. After observing no qualitative differences between the left and right saccades, adaptation trials in both directions were combined for analyses.

For the reaching adaptation task, the data was filtered using a dual-pass 6^{th} order low pass Butterworth filter with a cut-off frequency of 25 Hz. Movement onset and end were defined using a speed threshold of 3cm/s. Movements were included in the dataset if their duration was above 300ms, crossed at least once the target, and ended less than 3cm from the target center. Based on this criterion, we excluded in average 1.1% of the trials for NI participants (min: 0.3%, max: 2.3%) and 4.9% of the trials for ET patients (min: 0%, max: 21.1%). Adaptation was quantified using Pearson's correlation between the force orthogonal to straight path measured at the interface between the hand and the robot handle (measured force), and the force field commanded by the robot and extracted offline based on velocity signals of each trial (commanded force). Intuitively, if the measured force and the commanded force are equal and opposite, one expects high values of correlation between these signals. In contrast, a lack of knowledge of the force field producing only approximate or poorly tuned compensation for the perturbation should yield lower correlation values. It was also verified empirically that this metric was indeed sensitive to adaptation in the same setup and task (31). Initial angles, between the hand path and the straight line connecting the two targets, were computed at 200ms after movement initiation, with a counter-clockwise angle being defined as positive. We verified that there was no qualitative difference between the two targets, thus movements were remapped and combined for all analyses. We used a constant bin width of 8 trials for illustration purposes to show the effect of the perturbations.

Statistical Analysis

In both experiments, Student's t-tests were used to compare performances between groups during baseline condition (endpoint and maximum velocity of the saccade, movement duration, and

path length of the reaching movement) and for the initial angles from catch trials in the reaching adaptation task. T-tests were also used to compare average group age. Adaptation was evaluated using two techniques: exponential fits and Linear Mixed Effects (LME) models. A standard exponential model of adaptation was fitted on group average and 95% confidence intervals of each parameter were compared between ET and NI. The parameter *a* corresponds to the final offset to which the exponential curve converges, *b* is the amplitude of adaptation which therefore impacts the starting point of the curve, and *c* to the learning rate. The variable *i* was the trial number. The exponential fit was as follows:

$$y = a + b * e^{-c*i} . \quad (1)$$

Because the exponential fits were not significant in all cases, we also used linear mixed models to assess the evolution of the dependent variables across trials and group while taking inter-individual variance as a random factor. More precisely, LME models were fitted with factors *Trial Number (i)* and *Group* (2 level factor) as fixed predictors, and a random intercept to capture idiosyncrasy. LME and exponential fits were used for vertical end-point, vertical velocity, and saccades slopes in the first experiment, and maximum perturbation forces, normalized deviation, initial angle, and forces correlations in the second experiment. For each dependent variable the formulae of LME was:

$$Y_{ij} = \beta_0 + \beta_1 * i + \beta_2 * Group + \beta_3 * Group * i + b_j + \epsilon_{i,j} , \quad (2)$$

where Y_{ij} represents the dependent variable of trial number i from participant j, β_i are the coefficient of the fixed predictors including trial number, group (control or ET), and interaction between them, and b_j is the random intercept for participant j, and $\epsilon_{i,j}$ is the residual.

To measure the variability of the movements, we investigated several bins across the movement and kept the bin with the highest variability which corresponded to 20ms around the midpoint between peak velocity and target crossing for the reaching adaptation and 20ms around the midpoint between peak velocity and movement end for the saccadic adaptation. Variability of each person was computed using their movement in each block. We compared variability of participants using Wilcoxon rank-sum tests. For the unpaired comparisons between groups, due to the limited number of participants and the inherent variability of our populations we defined the significance threshold at 0.05. This includes Spearman's and Pearson's correlations, Wilcoxon rank-sum tests and Student's t-test. Concerning the LME, where all trials are considered we expect increased statistical power and

therefore assessed the significance of each effect using an F-test and a significance threshold of 0.005 (32, 33).

Finally, a linear support vector machine classifier was trained on the final performances of each participant in a 2-dimensional space that contained the learning indices that exhibited strong differences across trials and groups. The purpose of the classification technique was to quantify the overlap between the two groups in this two-dimensional space, however the accuracy of the model was still assessed based on leave-one-out cross-validation. In addition to quantifying the overlap between the distributions, the support vector machine was also used to illustrate that the boundary between the two groups separated the plane into overall better or worse performances in the two groups. All analyses were performed offline with Matlab 2020b. The data will be available in Zenodo following the publication of the article.

3. Results

Experiment 1: Saccadic Adaptation

We instructed participants to perform visually guided saccades to a target projected on a screen. The time course of a trial followed standard protocols of saccadic adaptation (22, 30): after an initial fixation delay, the target was projected, and participants initiated a saccade (Figure 1a&b). During movement, the goal target jumped vertically, inducing a terminal error that was gradually reduced as adaptation progressed. The experiment started with baseline trials, during which the target did not jump (see Methods). A total of 40 volunteers took part to this experiment, 20 Essential Tremor (ET) patients (14 F, 6 M) and 20 neurologically intact (NI) volunteers (14 F, 6 M). There was no significant difference in age between ET patients (M = 58.6, SD = 15.4) and NI volunteers (M=56.8, SD = 12.4); (t-test; t_{38}=-0.4013, p= 0.69). We assessed tremor severity in all participants using the Fahn-Tolosa-Marin Tremor Rating Scale (FTM-TRS). ET patients obtained an average score of 8.8 ± 5 (mean ± SD) points in part A assessing tremor amplitude and 14.6 ± 7.6 points for part B which assesses drawings and pouring (part B). The average score of NI participants was 1 ± 1.3 (part A) and 1.5 ± 1.7 (part B).

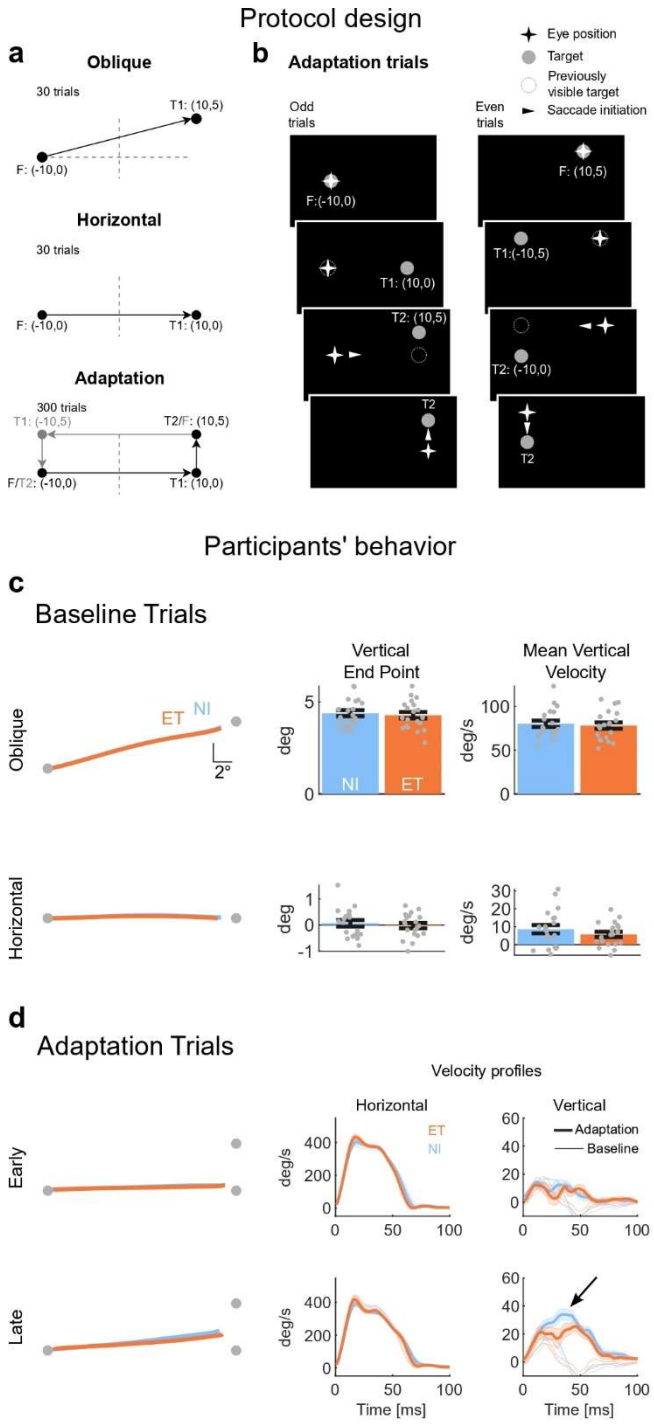

Figure 1 *Schematic representation of the saccadic adaptation protocol design **(a,b)** & behavior in saccadic adaptation task **(c,d).*** **a** Time course of a trial in the saccadic -adaptation task. A: Participants (n=40) were asked to perform saccades to gaze at a target visible on the screen. The experiment was divided into 3 trial types: oblique saccades, horizontal saccades, and adaptation saccades. Each trial began with a fixation target (F), followed by the appearance of the goal target (T1) after a random delay. Locations are indicated in visual degrees. During adaptation trials, the goal target was shifted by 5 degrees (T2). These trials occurred in two directions, to the right (black) and the left (grey). Target jump was counterclockwise. The dashed lines depict the axes centered straight ahead. **B** Target sequence from an adaptation trial. Arrows indicate when a saccade was initiated. Target jump (T1 to T2) occurs when the saccade is initiated. At the end of the trial, T2 served as fixation for the next trial (grey in 1A). **c** (Left) Group average of participants' eye trajectories averaged over the oblique and horizontal blocks. Grey dots represent the targets. (Right) Vertical end point and mean vertical velocity of saccades, across all trials, and averaged for the two groups. Error bars represent the SEM. Grey dots represent individual datapoints. **D** (Left) Saccades averaged over the first and last 10 trials to highlight differences between early and late adaptation phases. (Right) Average velocity traces are plotted for the horizontal and vertical components. Thin traces correspond to the horizontal baseline trials. Shaded areas represent the SEM.

The average eye trajectories of the baseline phase of the experiment are depicted in Figure 1c, left panel. No significant differences of vertical (t-tests; oblique: t_{38}=0.47, p=0.64; horizontal: t_{38}=0.55, p=0.58) and horizontal (t-tests; oblique: t_{38}=0.23, p=0.82; horizontal: t_{38}=0.79, p=0.43) end-point were observed between the two participants groups during these baseline trials. Likewise, average vertical (t-tests; oblique: t_{38}=0.39, p=0.7; horizontal: t_{38}=1.04, p=0.31) and horizontal (t-tests; oblique: t_{38}=-0.19, p=0.85; horizontal: t_{38}=-0.28, p=0.78) velocities were similar across the two groups. Mean velocity was computed on a 40ms window centered on the trial's peak velocity. No

statistical differences were observed regarding the fixation prior to the saccade, which was assessed by comparing averaged position and velocity across a 100ms window prior saccade initiation.

During the adaptation phase of the experiment, the target jumped vertically (5 visual degrees up/down) depending on the saccade direction (right/left respectively). The perturbation resulted in an endpoint error corrected by a second saccade. Both groups adapted their saccades to the target jump by increasing the vertical endpoint coordinate of the first saccade, but the extent of adaptation was significantly smaller for ET patients. The average eye trajectories at the beginning and the end of adaptation trials are plotted for each participant in Figure 1d. First, the vertical end-point of saccade increased with trial repetitions to reach an average of 2.06° (visual degrees) for NI participants, and only 1.83° for ET patients as can be seen in Figure 2a. Exponential fits were generally non-significant for the saccadic adaptation task (except for the 3rd slope), we therefore only present LME analyses for this task. A linear mixed-effect (LME) model revealed a significant main effect of the trial ($F_{(10,356)} = 24.20$, $p<10^{-4}$), no effect of the group (NI or ET) on the vertical end point was observed ($F_{(38)} =-0.44$, $p=0.66$) but there was a clear interaction effect between these two factors with a negative coefficient ($F_{(10,356)}=-5.22$, $p<10^{-4}$). This model shows that even if both groups started at the same level (no main effect, thus no offset on average) ET patients adapted at a lower rate to the perturbation than neurologically intact volunteers (interaction effect). The mean vertical velocity increased with trials for both groups, but with a smaller increase for the ET group (Figure 2b, LME; Trial : $F_{(10,356)} = 0.07$, $P<10^{-4}$; Group: $F_{(38)} = -2.16$, $P= 0.51$; Group-by-Trial : $F_{(10,356)} = -6.14$, $P<10^{-4}$). Participants performed a corrective saccade, in order to reach the final target T2. The amplitude of this saccade decreased with trial repetition, in accordance with the increase in the vertical endpoint coordinate of the first saccade. Similar to the first saccade, there was no group effect for the amplitude of the corrective saccade, but there was a significant interaction between the group and trial number, reflecting that ET patients adapted less to the perturbation (LME: Trial: $F_{(9497)} =-17.4$, $P<10^{-4}$; Group: $F_{(38)} =0.29$, $P=0.78$; Group:Trial: $F_{(9255)} =3.89$, $P<10^{-3}$).

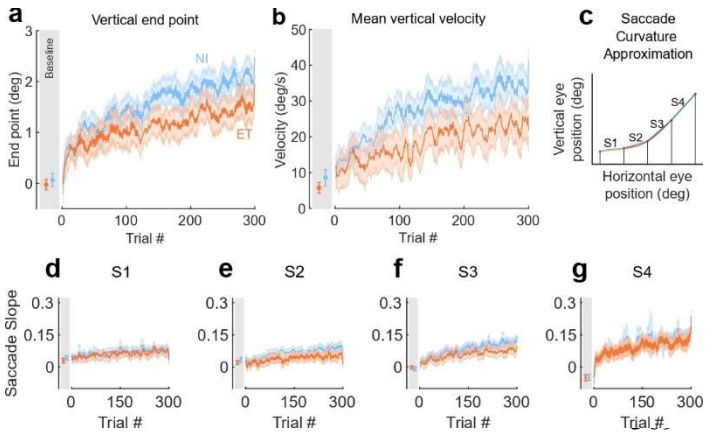

Figure 2 – *Participants' behaviour during the saccadic adaptation task*
ET patients showed reduced saccadic adaptation **a, b,** Evolution of the vertical end point (a) and peak vertical velocity (b) averaged over each group. Shading indicates SEM. **c,** The curvature was approximated by dividing saccade into 4 segments along the horizontal axis and by computing the slope of each segment (labeled S1 – S4). **d-g,** Evolution of the segment slopes with adaptation. **a,b,d-g**, grey area: Behavior in the horizontal baseline trials, error bars depicts the SEM.

Previous studies on saccadic adaptation (22, 30) reported a specific pattern in the evolution of saccades curvature, differentiating adapted saccades from oblique saccades with the same amplitude. Using the same technique, we approximated the saccade curvature by dividing the saccade into four equal segments along the horizontal axis and analyzed the evolution of the slope of each segment (S1-S4) (Figure 2c-g, see Methods). The differences between the slopes of segments is a proxy of the curvature since highly curved movements should display large variations in consecutive slopes. We observed an altered adaptation pattern in ET patients. The LME model revealed a significant effect of the trial and of the interaction between group and trial for all segments but the first one (LME; S1: Trial: $F_{(10,356)} = 8.41$, $p<10^{-4}$; Group: $F_{(38)} = -0.25$, $p=0.8$; Group-by-Trial: $F_{(10,356)}=-1.25$, $p=0.21$; For S2-S4 Trial: $F_{(10,356)} > 15.01$, $p<10^{-4}$; Group: $F_{(38)} > 0.09$, $p>0.24$; Group-by-Trial: $F_{(10,356)}<-2.88$, $p<0.004$). Differences between NI and ET participants were maximal during S2 and S3. Interestingly, the fact that the first segment of the saccade was similar across groups suggested the preservation of the initial component of saccadic adaptation -which could be seen as a proxy of anticipatory compensation-, whereas differences in S2 and S3 indicated impairment in the time course of saccadic execution supported by internal feedback. We studied whether any relationship existed between anticipation and real-time execution performances. For the patient group, we computed the correlation between the slope of the first segment and the end point, the correlation coefficient was 0.5 with a p-value of 0.03 (Spearman correlation). This relationship was expected as reported in Chen-Harris study where S1 was responsible of 75% of the total adaptation (30).

Finally, we compared the variability of participants' behaviour during the baseline blocks, and during the last trial of adaptation to observe participants' consistency during the task. We only report the results for the horizontal position, but similar results were observed for the other metrics (including vertical position as well as velocities in each direction). The variability was the most important towards the end of the movement, midway between peak horizontal velocity and the end

of the movement. For the horizontal, oblique and last block of adaptation, patients were respectively 28.8 %, 27.6% and 18.3% significatively more variable than controls (Wilcoxon rank-sum test: $T>489$, $z>2.12$, $p<0.03$). This variability was not correlated with the FTM-TRS score nor the task performance.

Experiment 2: Adaptation of reaching movements to a force field

For this experiment, we tested 20 ET patients (15 F, 5 M) and 20 NI participants (14 F, 6 M). The NI group was identical to the saccadic adaptation experiment, whereas the ET group involved 18 participants that were also tested in the saccadic adaptation task and 2 new participants. As for the saccadic adaptation task, we verified that there was no significant difference in age between the two groups (ET patients : M: 57.7, SD: 16.1, t-test: $t_{38}=-0.19$, $p=0.85$). ET patients obtained an FTM-TRS score of 9 ± 4.8 for part A (tremor amplitude) and 13.7 ± 6.5 for part B (drawings/pouring).

Participants first performed 40 movements moving the robotic handle of an instrumented device (KINARM, Kingston, ON) in a null field. These movements were used as control trials to measure differences between the two groups when no perturbation occurred (Figure 3a-d). We decomposed the trials into a reaching and a stabilization phase that were defined based on the time at which participant's hand crossed the target for the first time. The last movement of each participant in this field is depicted in grey in Figure 3f. The reaching phase was exempt of oscillations: movement duration and path length were similar for both groups (Figure 3e, t-test; Movement duration: $t_{38}=-0.16$, $p=0.87$; Path length: $t_{38}=-0.66$, $p=0.51$). The stabilization phase was, however, directly impacted by the tremor with longer movement duration and path length (Figure 3e, t-test; Movement duration: $t_{38}=-2.95$, $p=0.005$; Path length: $t_{38}=-3.3$, $p=0.002$). Initial assumptions were not made regarding differences between reaching and stabilization. Nevertheless for the subsequent analyses, we focused on the reaching phase of the movement – similar across groups in the absence of perturbation – as adaptation indices taken from this window would likely not be directly affected by the tremor.

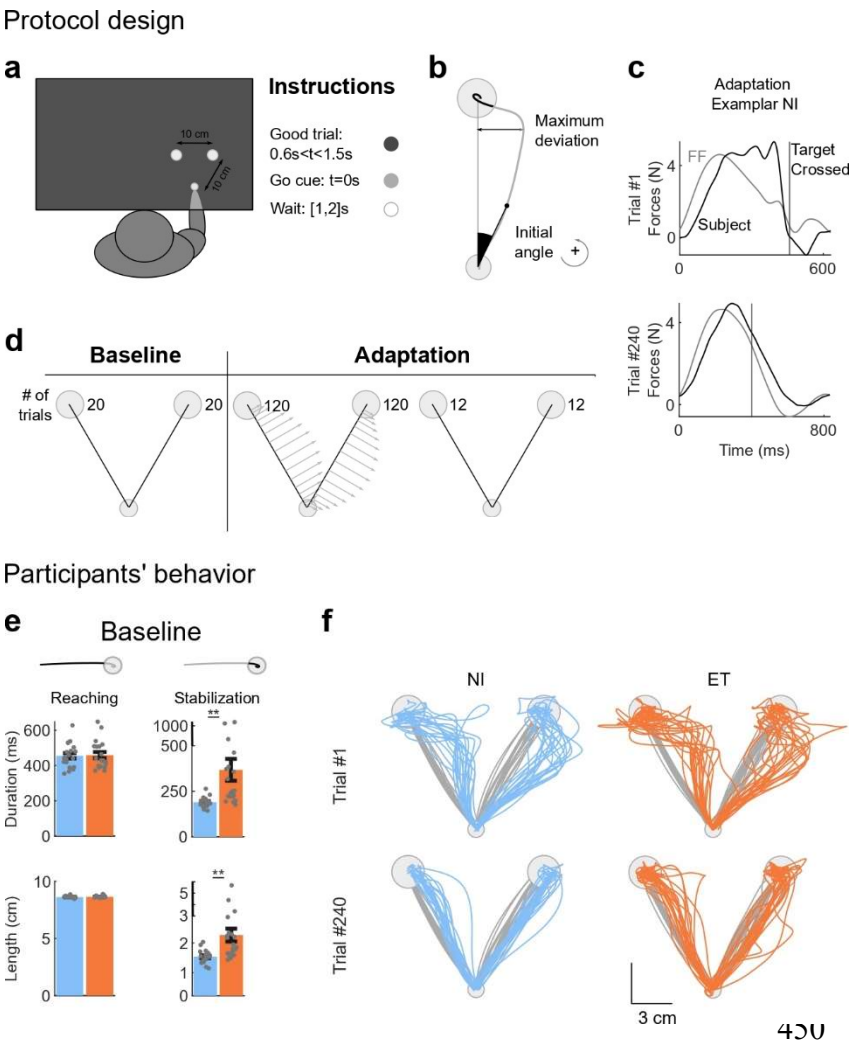

Figure 3 *Schematic representation of the upper limb adaptation protocol design **(a-d)** & Participants behavior during the reaching adaptation task **(e,f)**.* **a,** Participants (n=40) were asked to perform reaching movement to one of two goal targets displayed on the screen 10 cm away from the start target with hand-aligned cursor. Direct view of the limb was blocked. The timing of the movement was constrained, the go cue was given by the filling of the goal target. Visual feedback about movement timing was provided (see Methods). **B**, Parameters extracted from individual traces: the initial angle was defined as the angle between the straight line connecting the two targets and the hand position at 200ms. Counter-clockwise angle is defined as positive. Maximum deviation was computed between hand path and the straight line connecting the targets. **C,** Lateral Forces applied by participant on the handle (solid traces) and applied by the robot (grey traces) for an exemplar participant from the control group. Top and bottom panels illustrate the difference between early and late phases of the adaptation blocks. It can be observed that the applied force was closer to the perturbation force at the end of the adaptation phase. **D,** Time course of the protocol: 20 baseline trials towards each target (no force field). Adaptation trials were composed of 120 trials in each direction perturbed by a velocity dependent clockwise curl force field. Randomly interleaved catch trials (no force field) were included during the adaptation blocks. Target presentation order was randomized for each block. **E,** Movements were divided into reaching and stabilization. The end of reaching corresponded to the time at which the cursor crossed the target boundary. Significant differences between the two groups in movement duration and hand path lengths were observed only during the stabilization part. Error bars represent SEM. Note the modified scale for the stabilization measures. **F,** Participants' hand paths during the first (top) and last (bottom) force field trial. The differences between the trials illustrate adaptation. Grey traces correspond to the last baseline trial of each participant.

When participants were exposed to the force field for the first time, they all experienced large lateral hand deviations (Figure 3f). After a few trials, they quickly adapted their movements to the perturbation, and a reduction of the deviation relative to a straight line was observed: the path length decreased and the forces applied by the participant paralleled the one applied by the robot, a good compensation being the opposite of the perturbation (Figure 3c).

Similar to the saccadic adaptation task, both groups showed an adaptation of their movements to the force field, however, this adaptation was reduced for ET patients. The ET patients were slower in the task (Figure 4a&b; Movement duration – LME: Trial: $F_{(9255)}$ =-2.73, $P<10^{-2}$; Group: $F_{(38)}$ =2.19 , P=0.03 ; Group:Trial: $F_{(9255)}$ =-3.6 , $P<10^{-3}$). This resulted in a significantly smaller

perturbation (Figure 4c; LME: Trial: $F_{(9255)}$ =-13.11, $P<10^{-4}$; Group: $F_{(38)}$ =-1.65 , P=0.11 ; Group:Trial: $F_{(9255)}$ =6.62 , $P<10^{-4}$). To account for this difference, the maximum deviation measured during each trial (Figure 4d) was normalized by the maximum perturbation force during the trial. The normalized deviation (Figure 4e) was significantly higher in the ET group as revealed by the exponential fits, where all fitted parameters revealed reduced adaptation in the ET population (Figure 4e, asymptote (a) ET: a=0.33 (95% CI: 0.32-0.34), $P<10^{-4}$, NI: a=0.23 (0.22-0.24), $P<10^{-4}$, amplitude (b) ET: b=0.30 (0.24-0.37), $P<10^{-4}$, NI: b=0.21 (0.19-0.23), $P<10^{-4}$ and learning rate ET: c=0.10 (0.07-0.14), $P<10^{-4}$, NI: c=0.02 (0.015-0.025), $P<10^{-4}$). LME confirmed these results with a significant interaction between the group and the trial number (Figure 4e; LME: Trial: $F_{(9255)}$=-19.78, $P<10^{-4}$; Group: $F_{(38)}$ =0.91, P= 0.37; Group:Trial: $F_{(9256)}$=5.60, $P<10^{-4}$).

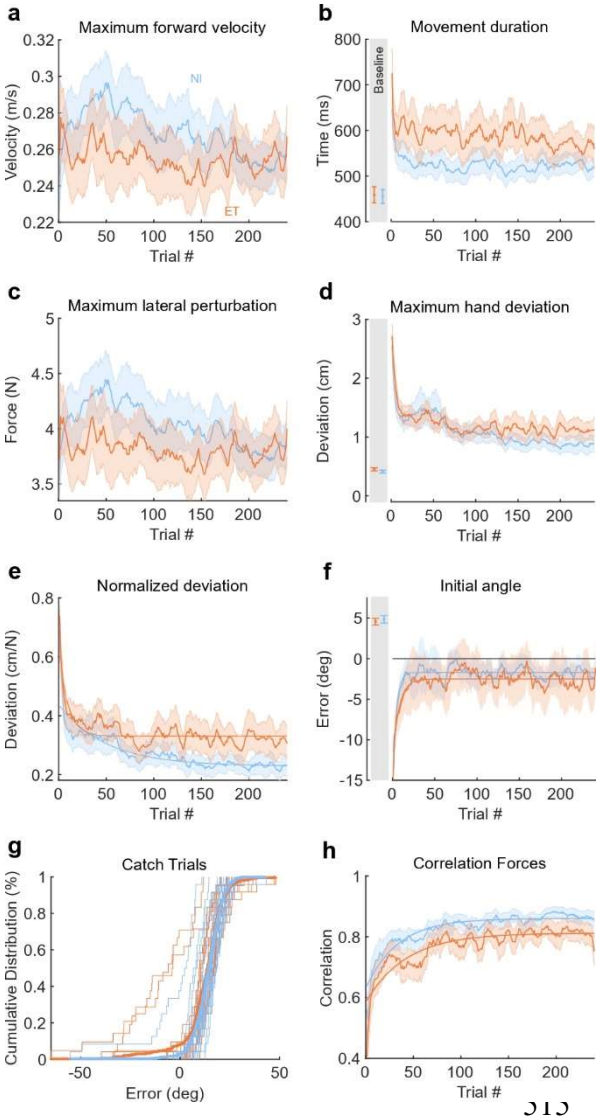

Figure 4 – *Participants' adaptation during the reaching task* **a,** Maximum forward velocity during the adaptation trials, used to compute the lateral perturbation. **b,** Movement duration during the reaching phase **c,** Maximum lateral perturbation received by the participants during the adaptation trials. Averaged over each group. **d,** Maximum hand deviation observed during force field trials. **e,** Maximum lateral deviation, normalized by the averaged force received during reaching. **f,** Initial angle between the hand and the line connecting the start-target centers at 200ms after movement initiation. **g,** Cumulative distribution of the initial angle during the catch trials for the ET and NI participants. **h,** Trial by trial correlation between the force field applied by the robot and the forces applied by the participant. Averaged over participants of each group. **a-f, h,** Shaded areas represent the SEM, grey area: average behavior in the baseline trials, error bars depicts the SEM. e,f,h: Significant exponential fits.

The initial reach angle is defined as the angle between the position of the hand at 200ms and the straight line connecting the home and the goal target (Figure 3b). It is a proxy of participants' anticipation of the perturbation as the earliest modulation of motor commands within movement was previously reported at ~250ms after movement onset (27, 31). It suggests that movement parameters prior to this time must be linked to anticipation. It is expected that the force field produces negative values of initial angles early in the adaptation phase, with gradual changes towards 0 as adaptation progresses. Exponential fits reported similar learning rates and amplitude for both groups but a significant difference in the asymptote (ET: a=-2.5 (95% CI: -2.8,-2.3), $P<10^{-4}$, NI: a=-1.7 (-1.9,-1.5), $P<10^{-4}$). Mixed models analyses reported a small difference in learning rate for the initial angles (Figure 4f), suggesting that both groups had slight differences in initial angles (LME: Trial: $F_{(9255)}=5.35$, $P<10^{-4}$; Group: $F_{(38)}=0.03$, P=0.98; Group:Trial: $F_{(9255)}=-3.40$, $P<10^{-3}$). However, no difference in initial angles was observed during the catch trials (Figure 4g; t-test; $t_{38}=0.83$, p=0.41). Similarly, the distributions were not significantly different (Kolmogorov-Smirnov test: D(38)=0.2, p=0.77). Overall, these results reflected no significant differences between the two groups in anticipating the perturbation.

In contrast, the compensation for the force field during movement was more strongly impacted. We computed the correlation between the perturbation force and the force measured at the handle, a high correlation highlighting a good compensation for the force field (31). We found an increase across trials for both groups, while remaining significantly smaller for ET patients than for NI participants (Figure 4h). Exponential fits reported a difference of asymptote (ET: a=0.81 (0.8-0.82), NI: a=0.86 (0.85-0.87)) and no significant differences in amplitude or learning rate. This result was also confirmed by LME models (Trial: $F_{(9020)}=20.41$, $P<10^{-4}$; Group: $F_{(37)}=-2.41$, P=0.021; Group:Trial: $F_{(9020)}=0.74$, P=0.46). Interestingly, the reaching adaptation experiment revealed impairments qualitatively similar to the saccadic adaptation task: first, ET patients were able to adapt, but they exhibited reduced adaptation in comparison with the control group. In both experiments, it appeared that the aspects linked to anticipation were preserved (S1 for the saccadic adaptation, the catch trials initial angles for the reaching task), whereas the metric closely linked to online execution exhibited a reduced compensation for the perturbation (S2 and S3 for the first task, and the correlations computed on continuous force traces for the reaching task). We did not find any significant correlation between the initial angle and the correlations (Spearman's correlation for the patient group; 0.38, p=0.12), suggesting an absence of interaction between both adaptation mechanisms.

We also compared participants' variability during the baseline block and the last block of adaptation. Variability peaked close to the end of the movement, midway between peak forward velocity and target crossing. During the baseline and the last block of adaptation, for the lateral velocity, ET patients were in average 51.4% and 49.6% significantly more variable than NI participants (Wilcoxon rank-sum test: $T>519$, $z>2.93$, $p<0.003$). This variability was not correlated with the FTM-TRS score nor the task performance. Similar results were observed for the lateral and forward position and velocity with a difference for the Spearman's correlations in the forward position where the variability positively correlated with the tremor score (Spearman correlation; baseline: 0.54, p=0.01, last block of adaptation: 0.45, p=0.046) and negatively with task performances during the baseline block (Spearman correlation; baseline: -0.75, $p<10^{-3}$, last block of adaptation: -0.46, p=0.057). We also observed trends in two other conditions for both comparisons ($p<0.10$).

Correlations between task performances and FTM-TRS scores

We investigated the correlation of tremor severity with the impairment for each task. Despite ET patients' significant impairment of saccadic adaptation, the FTM-TRS score (part A+B) was not correlated with the vertical end-point at the end of the adaptation (Figure 5a; Pearson's correlation = 0.11, p = 0.65). Concerning the force field adaptation task, a trend between the correlation of forces and the FTM-TRS score was observed (Figure 5b; Pearson's correlation = -0.47, p=0.047), suggesting that most affected ET patients were also those showing the larger impairment in reaching adaptation. It is clear that one participant with lowest task performance score both epitomizes and drives this effect. One the one hand, there was no anomaly with their data meaning that the result is likely valid. On the other hand, the correlation diminished to -0.40 with a p-value of 0.11 after removing this data point. In any case, additional data may be necessary to address the robustness of this relationship.

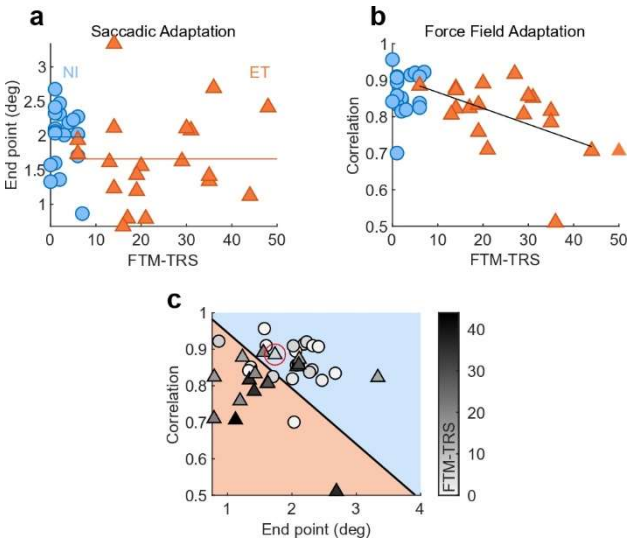

Figure 5 – Correlation between performance and tremor score

a, b, Relationship between the score obtained during late adaptation (**a**, Saccadic adaptation, **b**, Force field adaptation) and the Tremor Score measured via the FTM TRS scale (Part A+B). Each dot represents the average score obtained over the last 10% trials. **C,** Relationship between the performances in the two tasks for each participant. Color gradient represents the FTM TRS Score. The separation between the two groups was computed by training a linear support vector machine to discriminate populations based on the scores obtained in each task (accuracy: 67.6%). Red circle highlights a misclassification error for a less severely affected ET participant.

Finally, we sought to quantify the differences between the two-dimensional distributions of adaptation indices to measure the overlap across NI and patient's groups. We used a linear support vector machine, trained on the vertical end-point error and the continuous correlations, to visualize which task performances regions were associated with each group and quantify the overlap between the two populations taking two-dimensional linear separation in the space of adaptation indices. The classifier separated our performance space into reduced performances in both tasks for ET patients and higher performances in both tasks for NI volunteers, as shown in Figure 5c. In this dataset, participants classified in the blue region had an average FTM-TRS score of 7.1 points; participants classified in the orange region had an average score of 18.6 points. The support vector machine leave-one-out cross-validation accuracy was 67.6%. Classification errors mainly occurred for patients with a lower FTM-TRS score. Misclassifications happened more frequently for ET patients with lower FTM-TRS scores, closer to NI participants' scores. An example of misclassification for a less severely affected ET patient is highlighted on Figure 5c.

4. Discussion

Our study aimed to better understand the origin of the sensorimotor adaptation deficits previously reported in ET patients. To do so, we selected standard reaching and saccadic adaptation tasks known to be altered in patients with cerebellar deficits. As expected, ET patients experienced a deficit of adaptation in both tasks when compared with the control group. Importantly, our study revealed that the aspects linked to the anticipation of the perturbation, namely the initial saccade slope, the catch trials, and the initial reach angles, clearly evolved across trials and were intact for ET patients. In contrast the deficits seemed to be linked to markers of online control (intermediate saccade slopes and correlations in the reaching task).

Our results are consistent with previous adaptation studies performed with ET patients in various tasks (23–26). Here we reproduced the results of Chen et al. (23), and added to this line of evidence that the impairment in adaptation in ET patients may reflect a general sensorimotor deficit as it also impacts adaptation of saccades despite the absence of ET symptoms in unperturbed saccades (34, 35).

Although a linear correlation was not observed between the tremor score and the performance in the saccadic adaptation task, a trend was observed indicating that higher tremor score were related to lower performance in the force field adaptation task. This result might be explained by the fact that the FTM-TRS scale mostly evaluates upper limb sensorimotor function and tremor, whereas eye movements are not included or evaluated in this clinical scale. The overall tendency was an ordering of the patient's group in the region of the space of parameters used to quantify adaptation corresponding to lower performances in both tasks.

A previous study reported an interaction between noise and adaptation performances (36). They reported a decreased adaptation rate when execution noise (noise originating from the sensorimotor pathway) was more important and increased adaptation rate when planning noise was more important. A parallel can be made here between execution noise and the increased variability observed in the population with ET. Interestingly, a negative trend was observed between variability and task performances and a positive trend between variability and tremor score for half of the metrics studied in the reaching adaptation task.

Our study is not without limitation but they may not have a strong impact on our interpretations. First, participants did not stop their medications before the evaluation, which may influence the FTM-TRS score. Our analyses of the correlations between performance and the tremor score were computed based on this score, and might therefore suffer from the heterogeneity of patients and treatments. Severely affected patients with efficient treatments might have a lower tremor score than less severely affected patients and therefore have an impact on the correlations computed. Accounting for the medication was however difficult due to the variety of treatments and dosages taken by the participants. Studying sensorimotor deficits while taking medication into account is likely a challenge for prospective studies. Besides the heterogeneity inherent with clinical population and the diversity of treatments, our conclusions are still supported by the fact that the components of motor control prior to the adaptation tasks were similar across groups. Another point of attention concerns the performance of our classifier, which requires validation and should not be hastily generalized. The classifier was used here to quantify the overlap between two distributions, and not to perform prediction on unseen data. The performance of such an approach must be

validated with larger datasets before becoming a candidate test to improve the diagnosis of ET. Finally, previous work has reported the existence of cognitive or explicit strategies during adaptation to force fields accounting for a fraction of force produced against a force field (37). It is clear that the initial movement angle could be composed of an explicit component, however it was likely similar across groups and our data do not allow us to isolate it. In addition, the main deficit again was linked to movement control which is difficult to relate to a cognitive bias or strategy in both tasks. We believe that quantifying the contribution of explicit components in ET is an interesting topic for follow-up studies.

In contrast with cerebellar ataxia, patients who showed dramatic impairments and almost complete absence of adaptation in the tasks performed in this present study, ET patients showed only reduced adaptation in both tasks (20, 22). When comparing the results of the control group obtained by Xu-Wilson et al. with our control group, it must be noted that adaptation in this study appears to be slightly reduced. This difference could be potentially attributed to variations in the experimental setup and protocols. Our motivation to conduct the present study was to parse out potential cerebellar deficits in ET patients. However, it is important to keep in mind that even if cerebellum seems to be involved, it does not exclude other causes. A clear difficulty in documenting these cerebellar deficits was that cerebellum has been associated with a wide range of sensorimotor functions, including motor adaptation and control (18–22). A common ground between adaptation and control is the use of internal models that have been also associated with cerebellum (11–13). It is widely assumed that the brain uses these internal models to produce an estimation of the next state based on the current state estimate and the sensory feedback. This estimation is required to perform fast and accurate movements in an unpredictable environment despite sensorimotor noise and delayed sensory feedback. Online monitoring of the movement and corrections inflight linked to cerebellar mechanisms was shown in saccadic eye movements (38–42), as well as reaching movements (17). It is therefore possible that internal models for control hosted in cerebellum would be responsible for tremor and for reduced online compensation in adaptation tasks. Such internal models can take several forms, including aspects linked to sensorimotor coordination, as well as operations linked to timing representations (43–46). In this regard, it is known that oscillations, explaining the low frequency components of ET tremor, can arise in a system that incorrectly compensates for sensorimotor delays (47, 48). Thus, we suggest that tremor arises from incorrect internal models in cerebellum likely associated with delay compensation, producing the well documented oscillations and deficits in online control.

The possible dissociation between anticipation and online control is important for interpreting ET disorders, and also potentially on the underlying dysfunction of the cerebello-thalamo-cortical loop (7, 49). Our proposed interpretation is that the cerebello-thalamo-cortical pathway conveys an estimate of the state of the system that combines an efferent copy of motor commands with sensory feedback and current estimates that compensates for sensorimotor delays. When the movement was initiated from a static posture, errors had not yet accumulated and movement started in the correct direction, but later in the trial, the faulty delay compensation accumulates errors and the closed-loop system starts producing erroneous control signals potentially leading to oscillations. This view suggests a very specific cause of tremor in ET patients, which is linked to errors in real-time state-estimation based on internal feedback of motor commands. Orienting future research on online feedback control in ET should bring novel insights to validate or invalidate the hypothesis of impaired delay compensation as candidate root cause of oscillations in this population.

To conclude, our contribution is twofold: on the one hand we replicate the presence of cerebellar-dependent adaptation deficits in ET population, adding to the line of evidence that this disorder is linked to cerebellar dysfunction. On the other hand, we proposed a movement decomposition suggesting a specific functional consequence of the altered cerebellar pathways, which affects online control more than anticipation.

Supplemental Data:

Table S1 - Demographic and clinical data of ET patients: DOI: 10.6084/m9.figshare.24072213

5. References

1. **Louis ED**, **Ferreira JJ**. How common is the most common adult movement disorder? Update on the worldwide prevalence of essential tremor. *Mov Disord* 25: 534–541, 2010. doi: 10.1002/mds.22838.

2. **Bhatia KP**, **Bain P**, **Bajaj N**, **Elble RJ**, **Hallett M**, **Louis ED**, **Raethjen J**, **Stamelou M**, **Testa CM**, **Deuschl G**, **the Tremor Task Force of the International Parkinson and Movement Disorder Society**. Consensus Statement on the classification of tremors. from the task force on tremor of the International Parkinson and Movement Disorder Society: IPMDS Task Force on Tremor Consensus Statement. *Mov Disord* 33: 75–87, 2018. doi: 10.1002/mds.27121.

3. **Clark LN**, **Louis ED**. Essential tremor. Elsevier B.V.

4. **Shanker V**. Essential tremor: Diagnosis and management. *The BMJ* 366, 2019. doi: 10.1136/bmj.l4485.

5. **Ibrahim MF**, **Beevis JC**, **Empson RM**. Essential Tremor – A Cerebellar Driven Disorder? *Neuroscience* 462: 262–273, 2021. doi: 10.1016/j.neuroscience.2020.11.002.

6. **Mavroudis I**, **Petrides F**, **Karantali E**, **Chatzikonstantinou S**, **McKenna J**, **Ciobica A**, **Iordache AC**, **Dobrin R**, **Trus C**, **Kazis D**. A voxel-wise meta-analysis on the cerebellum in essential tremor. *Med Lith* 57: 1–10, 2021. doi: 10.3390/medicina57030264.

7. **Muthuraman M**, **Raethjen J**, **Koirala N**, **Anwar AR**, **Mideksa KG**, **Elble R**, **Groppa S**, **Deuschl G**. Cerebello-cortical network fingerprints differ between essential, Parkinson's and mimicked tremors. *Brain* 141: 1770–1781, 2018. doi: 10.1093/brain/awy098.

8. **Pietracupa S**, **Bologna M**, **Tommasin S**, **Berardelli A**, **Pantano P**. The Contribution of Neuroimaging to the Understanding of Essential Tremor Pathophysiology: a Systematic Review. *Cerebellum* , 2021. doi: 10.1007/s12311-021-01335-7.

9. **Tikoo S**, **Pietracupa S**, **Tommasin S**, **Bologna M**, **Petsas N**, **Bharti K**, **Berardelli A**, **Pantano P**. Functional disconnection of the dentate nucleus in essential tremor. *J Neurol* , 2020. doi: 10.1007/s00415-020-09711-9.

10. **Louis ED**, **Faust PL**. Essential tremor pathology: neurodegeneration and reorganization of neuronal connections. *Nat Rev Neurol* 16: 69–83, 2020. doi: 10.1038/s41582-019-0302-1.

11. **Diedrichsen J**, **Bastian AJ**. Cerebellar Function. .

12. **McNamee D**, **Wolpert DM**. Internal Models in Biological Control. *Annu Rev Control Robot Auton Syst* 2: 339–364, 2019. doi: 10.1146/annurev-control-060117-105206.

13. **Therrien AS**, **Bastian AJ**. Cerebellar damage impairs internal predictions for sensory and motor function. *Curr Opin Neurobiol* 33: 127–133, 2015. doi: 10.1016/j.conb.2015.03.013.

14. **Kilteni K**, **Engeler P**, **Ehrsson HH**. Efference Copy Is Necessary for the Attenuation of Self-Generated Touch. *iScience* 23: 100843, 2020. doi: 10.1016/j.isci.2020.100843.

15. **Miall RC**, **Weir DJ**, **Wolpert DM**, **Stein JF**. Is the Cerebellum a Smith Predictor? *J Mot Behav* 25: 203–216, 1993. doi: 10.1080/00222895.1993.9942050.

16. **Wolpert DM**, **Miall RC**, **Kawato M**. Internal models in the cerebellum. *Trends Cogn Sci* 2: 338–347, 1998. doi: 10.1016/S1364-6613(98)01221-2.

17. **Miall RC**, **Christensen LOD**, **Cain O**, **Stanley J**. Disruption of state estimation in the human lateral cerebellum. *PLoS Biol* 5: 2733–2744, 2007. doi: 10.1371/journal.pbio.0050316.

18. **Baizer JS**, **Kralj-Hans I**, **Glickstein M**. Cerebellar Lesions and Prism Adaptation in Macaque Monkeys. *J Neurophysiol* 81: 1960–1965, 1999. doi: 10.1152/jn.1999.81.4.1960.

19. **Ojakangas CL**, **Ebner TJ**. Purkinje cell complex and simple spike changes during a voluntary arm movement learning task in the monkey. *J Neurophysiol* 68: 2222–2236, 1992. doi: 10.1152/jn.1992.68.6.2222.

20. **Smith MA**, **Shadmehr R**. Intact ability to learn internal models of arm dynamics in Huntington's disease but not cerebellar degeneration. *J Neurophysiol* 93: 2809–2821, 2005. doi: 10.1152/jn.00943.2004.

21. **Tseng YW**, **Diedrichsen J**, **Krakauer JW**, **Shadmehr R**, **Bastian AJ**. Sensory prediction errors drive cerebellum-dependent adaptation of reaching. *J Neurophysiol* 98: 54–62, 2007. doi: 10.1152/jn.00266.2007.

22. **Xu-Wilson M**, **Chen-Harris H**, **Zee DS**, **Shadmehr R**. Cerebellar contributions to adaptive control of saccades in humans. *J Neurosci* 29: 12930–12939, 2009. doi: 10.1523/JNEUROSCI.3115-09.2009.

23. **Chen H**, **Hua SE**, **Smith MA**, **Lenz FA**, **Shadmehr R**. Effects of human cerebellar thalamus disruption on adaptive control of reaching. *Cereb Cortex* 16: 1462–1473, 2006. doi: 10.1093/cercor/bhj087.

24. **Bindel L**, **Mühlberg C**, **Pfeiffer V**, **Nitschke M**, **Müller A**, **Wegscheider M**, **Rumpf J-J**, **Zeuner KE**, **Becktepe JS**, **Welzel J**, **Güthe M**, **Classen J**, **Tzvi E**. Visuomotor Adaptation Deficits in Patients with Essential Tremor. .

25. **Hanajima R**, **Tsutsumi R**, **Shirota Y**, **Shimizu T**, **Tanaka N**, **Ugawa Y**. Cerebellar dysfunction in essential tremor. *Mov Disord* 31: 1230–1234, 2016. doi: 10.1002/mds.26629.

26. **Kronenbuerger M**, **Gerwig M**, **Brol B**, **Block F**, **Timmann D**. Eyeblink conditioning is impaired in subjects with essential tremor. *Brain* 130: 1538–1551, 2007. doi: 10.1093/brain/awm081.

27. **Mathew J**, **Crevecoeur F**. Adaptive Feedback Control in Human Reaching Adaptation to Force Fields. *Front Hum Neurosci* 15: 742608, 2021. doi: 10.3389/fnhum.2021.742608.

28. **Fahn S**, **Tolosa E**, **Marin C**. Clinical Rating Scale for Tremor. *Park Dis Mov Disord* 2: 271–280, 1993.

29. **Córdova Bulens D**, **Cluff T**, **Blondeau L**, **Moore RT**, **Lefèvre P**, **Crevecoeur F**. Different Control Strategies Drive Interlimb Differences in Performance and Adaptation during Reaching Movements in Novel Dynamics. *eneuro* 10: ENEURO.0275-22.2023, 2023. doi: 10.1523/ENEURO.0275-22.2023.

30. **Chen-Harris H**, **Joiner WM**, **Ethier V**, **Zee DS**, **Shadmehr R**. Adaptive control of saccades via internal feedback. *J Neurosci* 28: 2804–2813, 2008. doi: 10.1523/JNEUROSCI.5300-07.2008.

31. **Crevecoeur F**, **Thonnard JL**, **Lefèvre P**. A very fast time scale of human motor adaptation: Within movement adjustments of internal representations during reaching. *eNeuro* 7: 1–16, 2020. doi: 10.1523/ENEURO.0394-19.2019.

32. **Lakens D**, **Adolfi FG**, **Albers CJ**, **Anvari F**, **Apps MAJ**, **Argamon SE**, **Baguley T**, **Becker RB**, **Benning SD**, **Bradford DE**, **Buchanan EM**, **Caldwell AR**, **Van Calster B**, **Carlsson R**, **Chen S-C**, **Chung B**, **Colling LJ**, **Collins GS**, **Crook Z**, **Cross ES**, **Daniels S**, **Danielsson H**, **DeBruine L**, **Dunleavy DJ**, **Earp BD**, **Feist MI**, **Ferrell JD**, **Field JG**, **Fox NW**, **Friesen A**, **Gomes C**, **Gonzalez-Marquez M**, **Grange JA**, **Grieve AP**, **Guggenberger R**, **Grist J**, **Van Harmelen A-L**, **Hasselman F**, **Hochard KD**, **Hoffarth MR**, **Holmes NP**, **Ingre M**, **Isager PM**, **Isotalus HK**, **Johansson C**, **Juszczyk K**, **Kenny DA**, **Khalil AA**, **Konat B**, **Lao J**, **Larsen EG**, **Lodder GMA**, **Lukavský J**, **Madan**

CR, **Manheim D**, **Martin SR**, **Martin AE**, **Mayo DG**, **McCarthy RJ**, **McConway K**, **McFarland C**, **Nio AQX**, **Nilsonne G**, **De Oliveira CL**, **De Xivry J-JO**, **Parsons S**, **Pfuhl G**, **Quinn KA**, **Sakon JJ**, **Saribay SA**, **Schneider IK**, **Selvaraju M**, **Sjoerds Z**, **Smith SG**, **Smits T**, **Spies JR**, **Sreekumar V**, **Steltenpohl CN**, **Stenhouse N**, **Świątkowski W**, **Vadillo MA**, **Van Assen MALM**, **Williams MN**, **Williams SE**, **Williams DR**, **Yarkoni T**, **Ziano I**, **Zwaan RA**. Justify your alpha. *Nat Hum Behav* 2: 168–171, 2018. doi: 10.1038/s41562-018-0311-x.

33. **Benjamin DJ**, **Berger JO**, **Johannesson M**, **Nosek BA**, **Wagenmakers E-J**, **Berk R**, **Bollen KA**, **Brembs B**, **Brown L**, **Camerer C**, **Cesarini D**, **Chambers CD**, **Clyde M**, **Cook TD**, **De Boeck P**, **Dienes Z**, **Dreber A**, **Easwaran K**, **Efferson C**, **Fehr E**, **Fidler F**, **Field AP**, **Forster M**, **George EI**, **Gonzalez R**, **Goodman S**, **Green E**, **Green DP**, **Greenwald AG**, **Hadfield JD**, **Hedges LV**, **Held L**, **Hua Ho T**, **Hoijtink H**, **Hruschka DJ**, **Imai K**, **Imbens G**, **Ioannidis JPA**, **Jeon M**, **Jones JH**, **Kirchler M**, **Laibson D**, **List J**, **Little R**, **Lupia A**, **Machery E**, **Maxwell SE**, **McCarthy M**, **Moore DA**, **Morgan SL**, **Munafó M**, **Nakagawa S**, **Nyhan B**, **Parker TH**, **Pericchi L**, **Perugini M**, **Rouder J**, **Rousseau J**, **Savalei V**, **Schönbrodt FD**, **Sellke T**, **Sinclair B**, **Tingley D**, **Van Zandt T**, **Vazire S**, **Watts DJ**, **Winship C**, **Wolpert RL**, **Xie Y**, **Young C**, **Zinman J**, **Johnson VE**. Redefine statistical significance. *Nat Hum Behav* 2: 6–10, 2017. doi: 10.1038/s41562-017-0189-z.

34. **Helmchen C**, **Hagenow A**, **Miesner J**, **Sprenger A**, **Rambold H**, **Wenzelburger R**, **Heide W**, **Deuschl G**. Eye movement abnormalities in essential tremor may indicate cerebellar dysfunction. *Brain* 126: 1319–1332, 2003. doi: 10.1093/brain/awg132.

35. **Wójcik-Pędziwiatr M**, **Plinta K**, **Krzak-Kubica A**, **Zajdel K**, **Falkiewicz M**, **Dylak J**, **Ober J**, **Szczudlik A**, **Rudzińska M**. Eye movement abnormalities in essential tremor. *J Hum Kinet* 52: 53–64, 2016. doi: 10.1515/hukin-2015-0193.

36. **Van Der Vliet R**, **Frens MA**, **De Vreede L**, **Jonker ZD**, **Ribbers GM**, **Selles RW**, **Van Der Geest JN**, **Donchin O**. Individual Differences in Motor Noise and Adaptation Rate Are Optimally Related. *eneuro* 5: ENEURO.0170-18.2018, 2018. doi: 10.1523/ENEURO.0170-18.2018.

37. **Schween R**, **McDougle SD**, **Hegele M**, **Taylor JA**. Assessing explicit strategies in force field adaptation. *J Neurophysiol* 123: 1552–1565, 2020. doi: 10.1152/jn.00427.2019.

38. **Crevecoeur F**, **Kording KP**. Saccadic suppression as a perceptual consequence of efficient sensorimotor estimation. *eLife* 6: 1–15, 2017. doi: 10.7554/eLife.25073.

39. **Lefèvre P**, **Quaia C**, **Optican LM**. Distributed model of control of saccades by superior colliculus and cerebellum. *Neural Netw* 11: 1175–1190, 1998. doi: 10.1016/S0893-6080(98)00071-9.

40. **Quaia C**, **Lefèvre P**, **Optican LM**. Model of the Control of Saccades by Superior Colliculus and Cerebellum. *J Neurophysiol* 82: 999–1018, 1999. doi: 10.1152/jn.1999.82.2.999.

41. **Schreiber C**, **Missal M**, **Lefèvre P**. Asynchrony Between Position and Motion Signals in the Saccadic System. *J Neurophysiol* 95: 960–969, 2006. doi: 10.1152/jn.00315.2005.

42. **Xu-Wilson M**, **Tian J**, **Shadmehr R**, **Zee DS**. TMS Perturbs Saccade Trajectories and Unmasks an Internal Feedback Controller for Saccades. *J Neurosci* 31: 11537–11546, 2011. doi: 10.1523/JNEUROSCI.1584-11.2011.

43. **Bo J**, **Block HJ**, **Clark JE**, **Bastian AJ**. A Cerebellar Deficit in Sensorimotor Prediction Explains Movement Timing Variability. *J Neurophysiol* 100: 2825–2832, 2008. doi: 10.1152/jn.90221.2008.

44. **Diedrichsen J**, **Criscimagna-Hemminger SE**, **Shadmehr R**. Dissociating Timing and Coordination as Functions of the Cerebellum. *J Neurosci* 27: 6291–6301, 2007. doi: 10.1523/JNEUROSCI.0061-07.2007.

45. **Kilteni K**, **Houborg C**, **Ehrsson HH**. Rapid learning and unlearning of predicted sensory delays in self-generated touch. *eLife* 8: e42888, 2019. doi: 10.7554/eLife.42888.

46. **Martin TA**, **Keating JG**, **Goodkin HP**, **Bastian AJ**, **Thach WT**. Throwing while looking through prisms: I. Focal olivocerebellar lesions impair adaptation. *Brain* 119: 1183–1198, 1996. doi: 10.1093/brain/119.4.1183.

47. **Crevecoeur F**, **Gervers M**. Filtering compensation for delays and prediction errors during sensorimotor control. 2954: 2925–2954, 2019. doi: 10.1162/NECO.

48. **Stein RB**, **Oğuztöreli MN**. Tremor and other oscillations in neuromuscular systems. *Biol Cybern* 22: 147–157, 1976. doi: 10.1007/BF00365525.

49. **Helmich RC**, **Toni I**, **Deuschl G**, **Bloem BR**. The pathophysiology of essential tremor and parkinson's tremor. *Curr Neurol Neurosci Rep* 13, 2013. doi: 10.1007/s11910-013-0378-8.